INTERNATIONAL JOURNAL OF ENERGY RESEARCH
Int. J. Energy Res. 2006; **30**:861–873
Published online 10 April 2006 in Wiley InterScience (www.interscience.wiley.com). DOI: 10.1002/er.1191

Analytical and numerical investigation of the solar chimney power plant systems

Ming Tingzhen, Liu Wei*,†,‡ and Xu Guoliang

School of Energy and Power Engineering, Huazhong University of Science and Technology, Wuhan 430074, China

SUMMARY

There is a surge in the use of the solar chimney power plant in the recent years which accomplishes the task of converting solar energy into kinetic energy. As the existing models are insufficient to accurately describe the mechanism, a more comprehensive model is advanced in this paper to evaluate the performance of a solar chimney power plant system, in which the effects of various parameters on the relative static pressure, driving force, power output and efficiency have been further investigated. Using the solar chimney prototype in Manzanares, Spain, as a practical example, the numerical studies are performed to explore the geometric modifications on the system performance, which show reasonable agreement with the analytical model. Copyright © 2005 John Wiley & Sons, Ltd.

KEY WORDS: solar chimney power plant system; relative static pressure; driving force; natural convection

1. INTRODUCTION

The widespread use of solar energy, as an alternate and nondepletable resource for agriculture and industry as well as other applications, is dependent on the development of solar systems which possess the reliability, performance and economic characteristics that compare favourably with the conventional systems. The solar chimney power plant system, which is composed of the solar collector, the chimney and the turbine, has been investigated all over the world since the German researcher Jorg Schliaich first made the brainchild in the 1970s. The main objective of the collector is collecting solar radiation to heat up the air inside. As the air density inside the system is less than that of the environment at the same height, natural convection affected by buoyancy which acts as driving force comes into existence. Due to the existence of the chimney, the cumulative buoyancy results in a large pressure difference between the system and the environment, then the heated air rises up into the chimney with great speed.

*Correspondence to: Liu Wei, School of Energy and Power Engineering, Huazhong University of Science and Technology, Wuhan 430074, China.
†E-mail: w_liu@hust.edu.cn
‡Professor.

Contract/grant sponsor: National Key Basic Research Development Program; contract/grant number: G2000026303

Received 26 September 2005
Revised 17 October 2005
Accepted 16 November 2005

If an axis-based turbine is placed inside the chimney where there is a large pressure drop, the potential and heat energy of the air can be converted into kinetic energy and ultimately into electric energy.

After Schlaich's pioneer work on the solar chimney concept to harness solar energy, Haaf *et al*. (1983) provided fundamental investigations for the Spanish prototype system in which the energy balance, design criteria and cost analysis were discussed. Later, the same authors (1984) reported preliminary test results of the solar chimney power plant. Krisst (1983) demonstrated a 'back yard type' device with a power output of 10 W in West Hartford, Connecticut, U.S.A. Kulunk (1985) produced a microscale electric power plant of 0.14 W in Izmit, Turkey. Pasumarthi and Sherif (1998a) developed a mathematical model to study the effect of various environment conditions and geometry on the air temperature, air velocity, and power output of the solar chimney. Pasumarthi and Sherif (1998b) also developed three model solar chimneys in Florida and reported the experimental data to assess the viability of the solar chimney concept. Padki and Sherif (1999) developed a simple model to analyse the performance of the solar chimney. Lodhi (1999) presented a comprehensive analysis of the chimney effect, power production, efficiency, and estimated the cost of the solar chimney power plant set up in developing nations. Bernardes *et al*. (1999) presented a theoretical analysis of a solar chimney, operating on natural laminar convection in steady state. Gannon and Backstrom (2000) presented an air standard cycle analysis of the solar chimney power plant for the calculation of limiting performance, efficiency, and relationship between main variables including chimney friction, system, turbine and exit kinetic energy losses. Bernardes and Weinrebe (2003) developed a thermal and technical analysis to estimate the power output and examine the effect of various ambient conditions and structural dimensions on the power output. Pastohr *et al*. (2004) carried out a numerical simulation to improve the description of the operation mode and efficiency by coupling all parts of the solar chimney power plant including the ground, collector, chimney, and turbine. Schlaich and Weinrebe (2005) presented theory, practical experience, and economy of solar chimney power plant to give a guide for the design of 200 MW commercial solar chimney power plant systems. Ming *et al*. (2005) presented a thermodynamic analysis on the solar chimney power plant and advanced energy utilization degree to analyse the performance of the system. Liu *et al*. (2005) carried out a numerical simulation for the MW-graded solar chimney power plant, presenting the influences of pressure drop across the turbine on the draft and the power output of the system.

For a solar chimney power plant system with certain geometrical dimensions, the important factors which influence the power output are solar radiation, chimney height and volumetric flux which have been analysed and validated by theoretical and experiment investigations. However, the role of pressure difference on the performance of solar chimney systems has long been ignored. Many researchers only recognize the pressure difference as a function of the air density difference and the chimney height (Haff *et al*., 1983; Lodhi, 1999). Lodhi (1999) and Bernardes *et al*. (2003) neglected the theoretical analysis of pressure in the system but gave a comparatively simple driving force expression. Gannon and Backstrom (2000), Krisst (1983), Kulunk (1985), Pasumarthi and Sherif (1998a,b) and Padki and Sherif (1999) also ignored the discussion on pressure difference. Recently, Pastohr *et al*. (2004) presented pressure profiles of the collector numerically, but in his investigation the static pressure inside the collector is positive and increases along the flow direction, which is in contradiction with the basic flow theory and the solar chimney principle. Therefore, the effect of pressure difference on the performance of solar chimneys and the pressure field in the system remain unsolved problem, which motivate us to do

a thorough analysis on the pressure distribution, explore the relationship between the relative static pressure and driving force, and predict the power output and efficiency.

2. RELATIVE STATIC PRESSURE

Consider the static pressure profiles inside and outside the chimney as shown in Figure 1. Denoting by S the static pressure difference between the chimney and the environment at the same height:

$$S = p_{\mathrm{i}} - p_{\mathrm{o}}$$

Thereby, S can be regarded as the relative static pressure. Hence S at x and $x+\mathrm{d}x$ can be written as

$$S_x = p_{\mathrm{i},x} - p_{\mathrm{o},x} \tag{1}$$

$$S_{x+\mathrm{d}x} = S_x + \frac{\mathrm{d}S_x}{\mathrm{d}x}\,\mathrm{d}x \tag{2}$$

From the definition of S and the equations above, we have

$$\frac{\mathrm{d}S_x}{\mathrm{d}x} = \frac{\mathrm{d}p_{\mathrm{i},x}}{\mathrm{d}x} - \frac{\mathrm{d}p_{\mathrm{o},x}}{\mathrm{d}x} \tag{3}$$

In the environment, the relationship between the static pressure and air density can be written as

$$\frac{\mathrm{d}p_{\mathrm{o},x}}{\mathrm{d}x} = -\rho_{\mathrm{o},x} g \tag{4}$$

Considering a steady adiabatic solar chimney power plant system of cylindrical geometry and neglecting the viscous friction, we can write the momentum equation as

$$\frac{\mathrm{d}p_{\mathrm{i},x}}{\mathrm{d}x} = -\rho_{\mathrm{i},x} g \tag{5}$$

Substituting Equations (3)–(5) into Equation (2) yields:

$$\mathrm{d}S_x = S_{x+\mathrm{d}x} - S_x = (\rho_{\mathrm{o},x} - \rho_{\mathrm{i},x}) g\,\mathrm{d}x \tag{6}$$

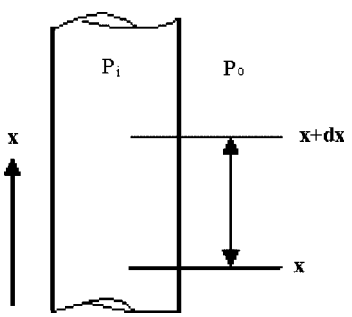

Figure 1. Static pressure inside and outside the chimney.

Integrating Equation (6) from 0 to x along the chimney yields:

$$S_x - S_0 = \int_0^x (\rho_{o,x} - \rho_{i,x}) g \, dx \tag{7}$$

At the chimney exit, the static pressure must be equal to the ambient atmospheric static pressure at that altitude. Thereby, we obtain

$$S_H = 0$$

Integrating Equation (7) we can obtain

$$S_0 = -(S_H - S_0) = -\int_0^H (\rho_{o,x} - \rho_{i,x}) g \, dx \tag{8}$$

For the small-scale solar chimney power plant systems, the density inside the chimney and the environment can be assumed to be constant. So Equation (8) can be written as

$$S_0 = -(\rho_o - \rho) g H \tag{9}$$

Substituting Equation (9) into Equation (7) yields:

$$S_x = -(\rho_o - \rho) g (H - x) \tag{10}$$

From Equations (9) and (10), we can easily find that, in the chimney, S has a negative value distribution. In addition, S has a linear relationship with the height of the chimney and the minimum value of S lies in the bottom of the chimney.

Although the expression of S is deduced in the chimney, it can also be used in the whole solar chimney power plant system. As the air is heated persistently inside the collector, the density may be less than that of the environment at the same height. Thus S also has a negative value distribution inside the collector.

In the collector, as the air velocity is not very large, the viscous resistance can be neglected. From the continuity equation and Bernoulli equation, we obtain

$$v_r = \frac{\dot{m}}{\rho A_r}$$

$$p_{i,r} + \rho_r g x + \tfrac{1}{2} \rho v_r^2 = \text{const}$$

As the height and velocity only change slightly along the flow direction inside the collector, the static pressure also changes slightly. But at the collector exit and the chimney inlet, as the flow section changes significantly, S may change significantly as well.

If the chimney is as high as 1000 m or higher, both the density inside the chimney and in the environment could not be regarded as constant. Thereby, introducing the so-called bulk air density in the system and the environment:

$$\rho_0 = \frac{\int_0^H \rho_{0,x} \, dx}{\int_0^H dx}, \quad \rho = \frac{\int_0^H \rho_{i,x} \, dx}{\int_0^H dx}$$

By using the bulk air densities in the deduction above, we can also get the similar form with Equations (9) and (10).

3. DRIVING FORCE

According to the above analysis, the minimum of S is the integration of pressure differences from the bottom to the chimney exit. As the system is connected with the environment by the collector inlet and the chimney exit, the pressure difference becomes the driving force to impel the air to flow inside the system. Thereby, according to Equation (9), we obtain

$$\Delta p = |S_{\min}| = |S_0| = (\rho_o - \rho)gH \tag{11}$$

Equation (11) indicates that the driving force is the absolute value of the relative static pressure at the bottom of the chimney, which can be expressed as the product of air density, gravity and the chimney height. Unfortunately, this expression cannot give detailed information of the factors which have effect on the driving force. As to different dimensions of solar chimney power plant systems, the collector radius, chimney radius and solar radiation can also have significant effect on the heating, temperature difference and air density difference. Hence, it is necessary to give a further discussion of Equation (11).

Taken into account the steady flow with constant solar radiation, radiation heat transfer between the walls and the air inside the system is converted into the convection heat transfer between the soil, canopy and the air. Evaluation of energy equilibrium along the radius of the collector and in the flow direction is carried out by dividing the collector several concentric sections. To one of the sections, the energy equilibrium equation can be written as

$$-c_p\dot{m}\frac{\mathrm{d}t_j}{\mathrm{d}r} = 2\pi r h_{g,a}(T_{g,j} - T_j) + 2\pi r h_{c,a}(T_{c,j} - T_j)$$

where $h_{g,a}$ and $h_{c,a}$ are the converted convective heat transfer coefficients of the soil and the canopy to the air, respectively. T_g and T_c are the temperature of the soil and canopy, respectively. Because the air flows to the centre of the collector, air temperature decreases with the increase of radius. Thereby there is a negative sign on the left-hand side of the equation. If we consider all the solar radiation is absorbed by the air inside the system, the energy can be converted to the heat transfer from the soil to the air:

$$-c_p\dot{m}\frac{\mathrm{d}T_j}{\mathrm{d}r} = (1 + C_1)2\pi r h_{g,a}(T_{g,j} - T_j) = q2\pi r$$

Then we integrate the equation above through the whole collector, the temperature profile along the collector can be written as

$$T - T_0 = \frac{\pi q}{c_p\dot{m}}(R_{coll}^2 - r^2) \tag{12}$$

where R_{coll} is the collector radius. It is noted that the maximum temperature difference in the collector should be when $r = 0$ in Equation (12).

The density difference may be expressed in terms of the volume coefficient of expansion, defined by:

$$\beta = \frac{\rho_0 - \rho}{\rho(T - T_0)} \tag{13}$$

Substituting Equations (12) and (13) into Equation (11), we obtain

$$\Delta p = \frac{\pi g\rho_0\beta_0 q}{c_p\dot{m}} H R_{coll}^2 \tag{14}$$

Neglecting the viscosity of the flow, and substituting the continuity equation and Bernoulli equation into Equation (14), we can obtain

$$\Delta p = \left(\frac{g^2}{2c_p}\right)^{1/3} \cdot \left(\frac{\rho_0^2 \beta_0^2}{\rho}\right)^{1/3} \cdot \left(\frac{H}{r_{\text{chim}}^2}\right)^{2/3} \cdot R_{\text{coll}}^{4/3} \cdot q^{2/3} \tag{15}$$

where r_{chim} is the chimney radius. From Equation (15), we can see that, for the natural convection in the solar chimney power plant system, the driving force depends on the chimney height and fluid properties. However, it also depends intensively on the solar radiation and the other dimensions such as the chimney radius and collector radius.

The driving force can be expressed by a function of the collector inlet, but to a certain solar chimney power plant, the collector inlet changes very little.

4. POWER OUTPUT AND EFFICIENCY

After successfully derived the expression of the driving force, we can easily obtain the expressions of other solar chimney performance parameters.

Substituting Equation (15) to Equation (14), we can get the mass flow rate:

$$\dot{m} = \pi \left(\frac{2g\rho\rho_0\beta_0}{c_p}\right)^{1/3} \cdot H^{1/3} \cdot r_{\text{chim}}^{4/3} \cdot R_{\text{coll}}^{2/3} \cdot q^{1/3} \tag{16}$$

The maximum power output can be expressed as the product of driving force and the volumetric flow rate:

$$P_{\max} = \frac{\Delta p \dot{m}}{\rho}$$

Substituting Equation (14) to the equation above yields:

$$P_{\max} = \frac{\rho_0}{\rho} \frac{\pi g}{c_p T_0} H R_{\text{coll}}^2 q \tag{17}$$

Equation (17) shows that the air properties, the chimney height, the collector radius and the solar radiation have significant effect on the maximum power output. Compared with the formulation advanced by Haaf *et al.* (1983), Equation (17) gives a detailed description of factors which influence the maximum power output.

The maximum efficiency of the system can be expressed by

$$\eta_{\max} = \frac{P_{\max}}{Q} = \frac{P_{\max}}{\pi R_{\text{coll}}^2 q}$$

Substituting Equation (17) to the equation above, we obtain

$$\eta_{\max} = \frac{\rho_0}{\rho} \frac{gH}{c_p T_0} \tag{18}$$

Equation (18) demonstrates the functional dependence of the system maximum efficiency on the air density, the inlet temperature and the chimney height. Equation (18) gives a more accurate expression of the maximum efficiency of the system compared with the results by Schlaich and Weinrebe (2005) and Gannon and Backstrom (2000).

5. RESULTS AND DISCUSSIONS

To validate the theoretical analysis, the relative static pressure distributions are compared with the numerical simulation results of the prototype in Manzanares, Spain. Later, solar chimney models with different geometrical parameters have been simulated to obtain the flow and temperature contours. During the simulation, the conservation equations for mass, momentum and energy, and standard κ–ε turbulent equations are selected (Tao, 2001), and natural convection and gravity effect are taken into consideration. The main boundary conditions are shown in Table I for energy conservation equations, and the temperature profiles of the ground and the canopy are different parabolic functions of the radius, and the functions will vary with different solar radiations.

Figures 2 and 3 show, when the solar radiation is $800\,\mathrm{W\,m^{-2}}$, the results of 3D numerical simulations, which are the axis section velocity distributions of the Spanish prototype. From Figure 2, a large swirl which lies in the collector outlet causes very small velocity, large pressure

Table I. Boundary conditions and model parameters.

Place	Type	Value
Surface of the ground	Wall	$T = f(r)$ K
Surface of the canopy	Wall	$T = g(r)$ K
Surface of the chimney	Wall	$q_{\mathrm{chim}} = 0\,\mathrm{W\,m^{-2}}$
Inlet of the collector	Pressure inlet	$S = 0$ Pa, $T_0 = 293.15$ K
Outlet of the chimney	Pressure outlet	$S = 0$ Pa

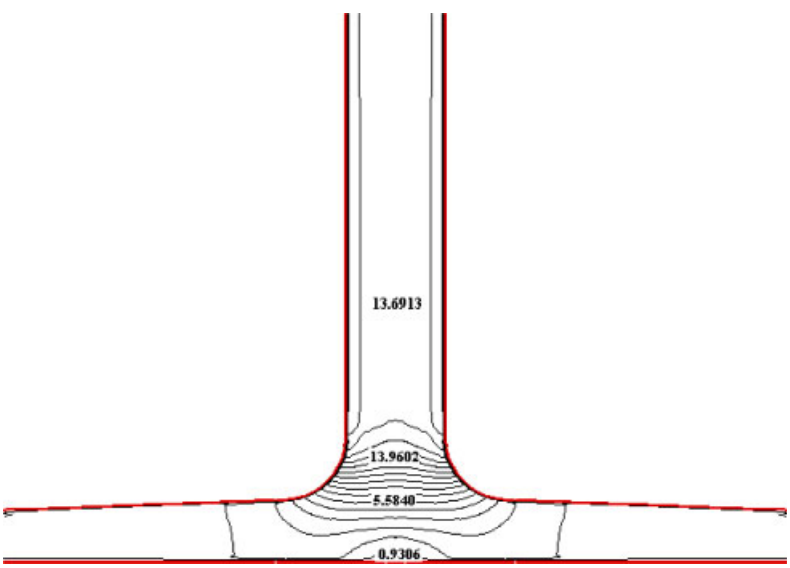

Figure 2. Velocity distribution in the Spanish prototype ($\mathrm{m\,s^{-1}}$).

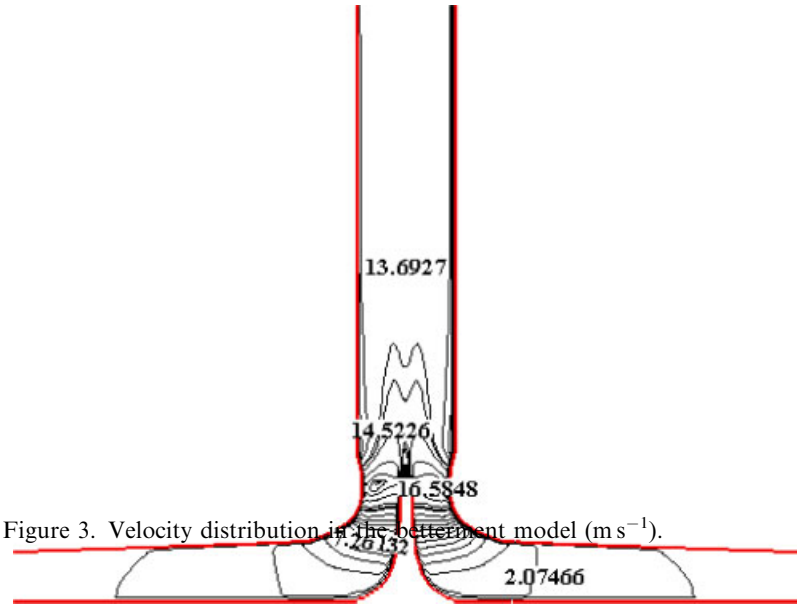

Figure 3. Velocity distribution in the betterment model ($m\,s^{-1}$).

and high temperature, which will cause large energy losses of the system. Thereby, a modification of the prototype model shown in Figure 3 was done to achieve a much larger velocity distribution. As a result, the local relative static pressure and velocity change significantly at the bottom of the chimney, but the main velocity in the chimney has no appreciable changes. The results suggest that it is feasible to increase the power output by modifying the local configuration of the solar chimney power plant.

Figure 4 is the numerical simulation results, which show that, when the solar radiation is $1000\,W\,m^{-2}$, the upwind velocity inside the chimney reaches about $16\,m\,s^{-1}$, and the temperature difference of the system with no-load condition simulation surpasses 20°C. The results are a little larger than the technical data only because it is supposed in this analytical model that the solar radiation is fully absorbed by the air inside the system. Thereby, we can see that the calculations done on the numerical simulation are consistent with the technical data of the Spanish prototype (Haff *et al.*, 1983).

Figure 5 shows the relative static pressure profiles with different collector radius but the same chimney height, in which the profile marked $R = 120$ is the prototype of the Spanish model and the profiles in the $0 < H < 10\,m$ range lie in the collector. From this figure, the minimum relative static pressure decrease with the increase of the collector radius, and the minimum values lie in the bottom of the chimney. When the collector radius is 200 m, the minimum relative static pressure is less than $-220\,Pa$. In addition, the relative static pressure increases along the chimney height, which shows great agreement with Equation (10).

Figure 6 show the influence of solar radiation and collector radius on the driving force of the system. When the solar radiation is constant, with the increase of the collector radius, the area of the air collector increases, the air temperature in the system increases which results in the decrease of the air density. Thereby, the relative static pressure in the system increases, and the driving force increases accordingly. Similarly, when the solar radiation increases, the air density will decrease for the same solar chimney model, and the driving force will also increase.

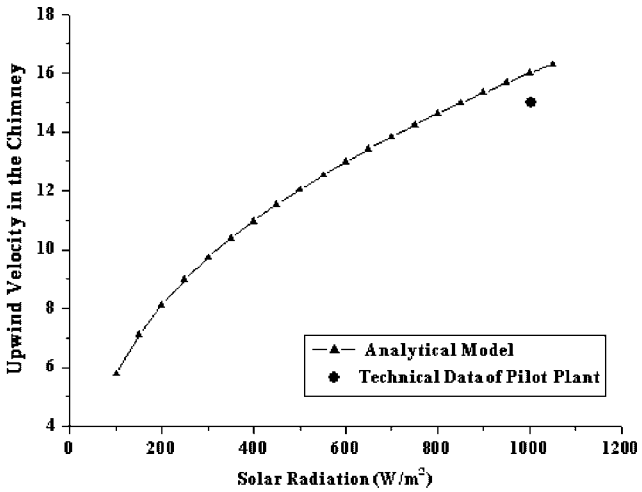

Figure 4. Comparison of velocity between analytical model and technical data.

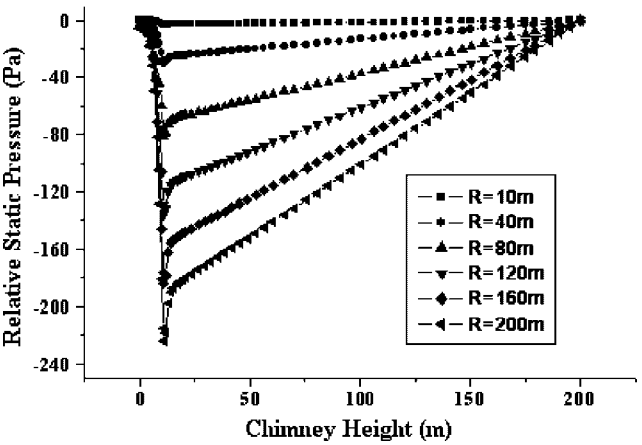

Figure 5. The effect of collector radius on the relative static pressure.

Figure 7 shows the effect of solar radiation and the chimney height on the power output of the system. As analysed above, when the solar radiation is constant, an increase of the chimney height causes an increase of the mass flow rate, and the driving force as well. The driving force can be used to drive the axis-based turbine. The increase of driving force will result in the increase of the pressure difference across the turbine. Therefore, the chimney height has a direct effect on the power output of the system. Figure 7 shows reasonable agreement with Equation (17).

Figures 8 and 9 show the effect of collector radius and the chimney height on the system efficiency. The curves of the former efficiency in these figures were obtained according to the formulation advanced by Schlaich and Weinrebe (2005) and Gannon and Backstrom (2000).

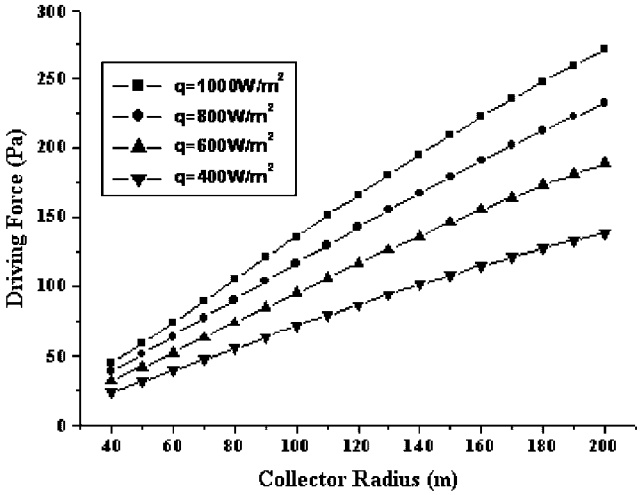

Figure 6. The effect of collector radius on the driving force.

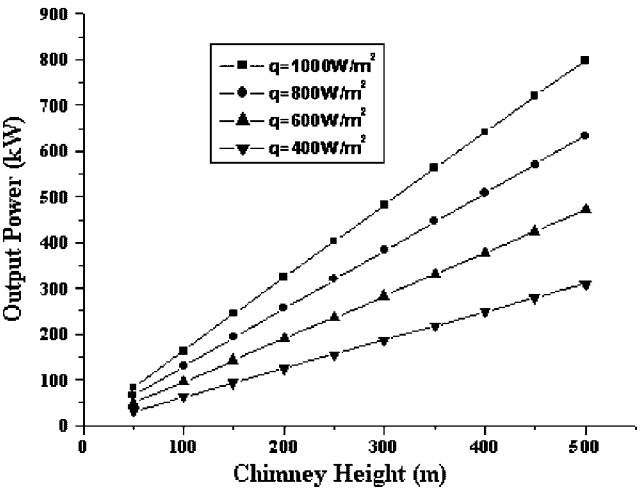

Figure 7. The effect of chimney height on the power output.

The former efficiency advanced by Schlaich and Gannon can be influenced only by the chimney height as shown, but it is indicated in the following two figures that the solar radiation and the collector radius can also have effect on the maximum efficiency advanced in this paper. The maximum efficiency will increase with the increase of solar radiation and collector radius.

However, it is easy to see from Figure 9 that the chimney height has a significant effect on the maximum efficiency. When the chimney height reaches 300 m and the solar radiation is 1000 W m^{-2}, the maximum efficiency will reach 1%, and it will surpass 3% when the chimney height reaches 1000 m. The efficiency of the 200 MW commercial solar chimney power plant system shown by Schlaich and Weinrebe (2005) is about 1%, so the maximum efficiency in

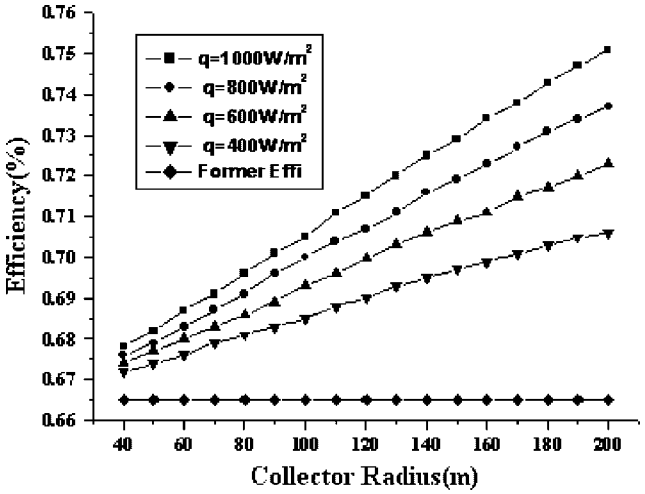

Figure 8. The effect of collector radius on the efficiency.

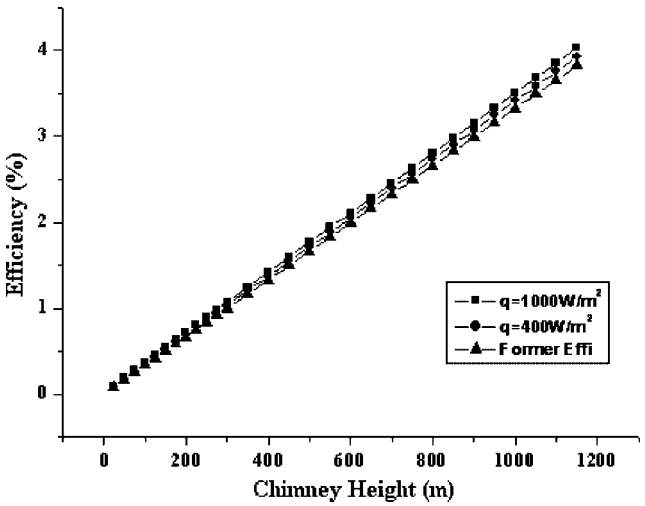

Figure 9. The effect of chimney height on the efficiency.

this paper gives an ideal limiting value for the design of large scale solar chimney power plant system.

In addition, the numerical simulation results also show the influence of chimney radius on the relative static pressure, driving force, power output and the system efficiency. When the solar radiation is constant, the effect of chimney radius on the performance of the solar chimney power plant is complicated: the increase of chimney radius will cause the increase of mass flow rate, but the increase of air density and the decrease of the driving force as well. This latter effect overshadows the effect of mass flux increase. Therefore, the power output and efficiency decrease slightly with the increase of the chimney radius.

6. CONCLUSIONS

This paper presents a detailed description of the relative static pressure, driving force, power output and efficiency as dependent on the effects of various parameters such as the chimney height and radius, collector radius and solar radiation. Contrary to the results shown by Pastohr *et al.* (2004), the relative static pressure is negative, and it decreases along the flow direction inside the collector but increases inside the chimney.

The results also show that driving force not only depends on the chimney height, but also on the solar radiation and the other system dimensions. Similarly, the maximum power output and maximum efficiency, compared with the results shown by Schlaich and Weinrebe (2005) and Gannon and Backstrom (2000), are also functions of the solar radiation and system dimensions besides the chimney height. When the chimney height reaches 300 m and the solar radiation is about $1000\,\mathrm{W\,m^{-2}}$, the maximum efficiency will reach 1%, and it will surpass 3% when the chimney height reaches 1000 m.

NOMENCLATURE

A = area ($\mathrm{m^2}$)
c_p = specific heat capacity of the air, 1005 ($\mathrm{J\,kg^{-1}\,K^{-1}}$)
g = gravity, 9.81 ($\mathrm{m\,s^{-2}}$)
h = heat transfer coefficient ($\mathrm{W\,m^{-1}\,K^{-1}}$)
H = chimney height (m)
$\dot{m}$ = mass flow rate (kg s)
Δp = driving force (Pa)
q = solar radiation ($\mathrm{W\,m^{-2}}$)
q_{chim} = heat flux through the chimney wall ($\mathrm{W\,m^{-2}}$)
r_{chim} = the chimney radius (m)
R_{coll} = collector radius (m)
S = relative static pressure (Pa)
T = temperature (K)
T_0 = temperature of the environment (K)
v = air velocity ($\mathrm{m\,s^{-1}}$)
x = coordinate in axial direction (m)

Greek letters

β = the volume coefficient of expansion ($\mathrm{K^{-1}}$)
ρ = air density ($\mathrm{kg\,m^{-3}}$)

ACKNOWLEDGEMENT

This work was supported by the National Key Basic Research Development Program of China (No. G2000026303).

REFERENCES

Bernardes MA, Vob A, Weinrebe G. 2003. Thermal and technical analyzes of solar chimneys. *Solar Energy* **75**:511–524.
Bernardes MADS, Valle RM, Cortez MF-B. 1999. Numerical analysis of natural laminar convection in a radial solar heater. *International Journal of Thermal Science* **38**:42–50.
Gannon AJ, Backstrom TW. 2000. Solar chimney cycle analysis with system loss and solar collector performance. *Journal of Solar Energy Engineering* **122**:133–137.
Haaf W, Friedrich K, Mayer G, Schlaich J. 1983. Solar chimneys. *International Journal of Solar Energy* **2**:3–20.
Haaf W, Friedrich K, Mayer G, Schlaich J. 1984. Solar chimneys. *International Journal of Solar Energy* **2**:141–161.
Kulunk H. 1985. A prototype solar convection chimney operated under Izmit conditions. *Proceedings of the 7th Miami International Conference on Alternative Energy Sources*, Veiroglu TN (ed.), vol. 162.
Krisst RJK. 1983. Energy transfer system. *Alternative Sources of Energy* **63**:8–11.
Liu W, Ming TZ, Yang K, Pan Y. 2005. Simulation of characteristic of heat transfer and flow for MW-graded solar chimney power plant system. *Journal of Huazhong Universidy of Science and Technology* **33**(8):5–7.
Lodhi MAK. 1999. Application of helio-aero-gravity concept in producing energy and suppressing pollution. *Energy Conversion and Management* **40**:407–421.
Ming TZ, Liu W, Xu GL, Yang K. 2005. Thermodynamic analysis of solar chimney power plant system. *Journal of Huazhong Universidy of Science and Technology* **33**(8):1–4.
Padki MM, Sherif SA. 1999. On a simple analytical model for solar chimneys. *International Journal of Energy Research* **23**:345–349.
Pastohr H, Kornadt O, Gurlebeck K. 2004. Numerical and analytical calculations of the temperature and flow field in the upwind power plant. *International Journal of Energy Research* **28**:495–510. DOI:10.1002/er.978.
Pasumarthi N, Sherif SA. 1998a. Experimental and theoretical performance of a demonstration solar chimney model—Part I: mathematical model development. *International Journal of Energy Research* **22**:277–288.
Pasumarthi N, Sherif SA. 1998b. Experimental and theoretical performance of a demonstration solar chimney model—Part II: experimental and theoretical results and economic analysis. *International Journal of Energy Research* **22**:443–461.
Schlaich J. 1995. *The Solar Chimney*. Edition Axel Menges: Stuttgart, Germany.
Schlaich J, Weinrebe G. 2005. Design of commercial solar updraft tower systems-utilization of solar induced convective flows for power generation. *Journal of Solar Energy Engineering* **127**:117–124. DOI:10.1115/1.1823493.
Tao WQ. 2001. *Numerical Heat Transfer* (2nd edn). Xi'an Jiaotong University Press: Xi'an, China.

